



CHORUS

This is the accepted manuscript made available via CHORUS. The article has been published as:

Predicting Complex Relaxation Processes in Metallic Glass

Yang Sun, Si-Xu Peng, Qun Yang, Feng Zhang, Meng-Hao Yang, Cai-Zhuang Wang, Kai-Ming Ho, and Hai-Bin Yu

Phys. Rev. Lett. **123**, 105701 — Published 6 September 2019

DOI: [10.1103/PhysRevLett.123.105701](https://doi.org/10.1103/PhysRevLett.123.105701)

Predicting Complex Relaxation Processes in Metallic Glass

Yang Sun,^{1,*} Si-Xu Peng,^{2,*} Qun Yang,² Feng Zhang,¹ Meng-Hao
Yang,¹ Cai-Zhuang Wang,¹ Kai-Ming Ho,¹ and Hai-Bin Yu^{2,†}

¹Ames Laboratory, US Department of Energy and Department of Physics, Iowa State University, Ames, Iowa 50011, USA

²Wuhan National High Magnetic Field Center and School of Physics,
Huazhong University of Science and Technology, Wuhan, Hubei 430074, China

Relaxation processes significantly influence the properties of glass materials. However, understanding their specific origins is difficult, even more challenging is to forecast them theoretically. In this study, using microseconds molecular dynamics simulations together with an accurate many-body interaction potential, we predict that an Al₉₀Sm₁₀ metallic glass would have complex relaxation behaviors: In addition to the main (α) relaxation, the glass (i) shows a pronounced secondary (β) relaxation at cryogenic temperatures and (ii) exhibits an anomalous relaxation process (α_2) accompanying α relaxation. Both of the predictions are verified by experiments. Computational simulations reveal the microscopic origins of relaxation processes: while the pronounced β relaxation is attributed to the abundance of string-like cooperative atomic rearrangements, the anomalous α_2 process is found to correlate with the decoupling of the faster motions of Al with slower Sm atoms. The combination of simulations and experiments represents a first glimpse of what may become a predictive routine and integral step for glass physics.

Compared with crystals, glasses inherently feature diverse relaxation dynamics over a wide range of temperature and timescales. These relaxation processes significantly influence properties of glass materials and are related to a number of crucial unresolved issues in glassy physics [1–5]. Understanding how the atomic rearrangements govern these processes represents an outstanding issue in glass physics [1, 3, 4, 6, 7].

Usually, the most prominent relaxation process is the primary (α) relaxation which is responsible for the vitrification of glass-forming liquid. Its falling out of equilibrium indicates the glass transition phenomenon. Processes occurring in addition to the α relaxation at shorter timescales or lower temperature are referred as secondary (β) relaxations. The studies over the last a few decades have established that the β relaxation could have important consequences on the mechanical properties for metallic and polymeric glasses, as well as thermal stability of glassy pharmaceuticals and biomaterials, and thus attract considerable attentions [8–13]. Moreover, recent studies have discovered there might be more relaxation processes in addition to the α and β relaxations in glasses [7, 14–20, 23]. Even the structurally simplest metallic glasses (MGs, compared to molecular and polymeric glasses) could exhibit multiple relaxations, indicating that a far richer-than-expected scenario for glass relaxation. For example, Wang *et al.* [17] and Kchemann *et al.* [15] identified a new relaxation process that is faster than the β relaxation in MGs which was named β' and γ relaxations. Wang *et al.* [21] also illustrate the β' relaxation might be correlated with the initiation of plastic deformation in MGs. Luo and coworkers [16] reported the non-equilibrium α relaxation would split into two processes in deep glassy state which causes early decay in the stress-relaxation experiments [22]. While these results illustrate that MGs possess complex relaxation

phenomena and have consequences on properties, it is difficult to understand their specific origins because of the lack of microscopic data of these processes.

In principle, molecular dynamics (MD) simulation is a powerful tool to investigate detailed atomic rearrangements in the glass relaxations at the microscopic level. However, the relaxations in the glassy states are extremely complicated, as they are sensitive to chemical compositions [24] and thermal histories [25, 26]. The related relaxation timescales (e.g., milliseconds to seconds) are usually several decades longer than the current available computational timescales (picoseconds to nanoseconds). It is therefore challenging to model the relaxation dynamics of realistic glass materials under experimental conditions. Moreover, for large-scale MD simulations of MGs, the force field which describes the many-body interactions (i.e., empirical potentials) is of vital importance [27–29]. Although there are a few potentials that can reproduce some static structural features and thermodynamics of MGs, their capability of describing dynamical processes is mostly unknown.

Recently, a realistic interaction potential for the study of Al₉₀Sm₁₀ MG was developed [30]. It correctly describes the glass structure [31], complex devitrification behaviors [32, 33] and crystal growth [34] in the Al-Sm systems. It also brings insights to the competition of crystallization and glass formation [35, 36]. Therefore, it provides a model system to investigate the relaxation mechanism in the realistic MG.

In this work, relying on this accurate interaction potential, we simulate the dynamical mechanical spectroscopy (DMS) of Al₉₀Sm₁₀ MG in the timescale up to 10 microseconds which almost reaches the limit of state-of-the-art computational power. With such a slow frequency, we find an anomalous relaxation process (noted as α_2) decouples from α relaxation. The MG also ex-

hibit a strongly pronounced β relaxation even on the MD timescale. The behaviors predicted from the MD simulations are verified with DMS experiments at cryogenic temperatures. The detailed atomic motions that lead to the relaxation processes are revealed from the MD trajectories. The feasibility that atomic simulations could discover new relaxation processes in MGs and elucidate their underlying mechanisms would be useful for understanding the dynamics and properties as well as the design of glass materials.

Simulation - MD simulations were carried out based on a Finnis-Sinclair potential [30], using the GPU-version of LAMMPS code [38–40]. The $\text{Al}_{90}\text{Sm}_{10}$ glass model, containing 32,000 atoms, were obtained by the continuous cooling with a cooling rate of 10^8K/s . The MD simulations of DMS (MD-DMS) [37] were performed during the cooling process, covering a wide temperature range from deeply undercooled liquid to low-temperature glass. In MD-DMS, a sinusoidal strain was applied with an oscillation period t_ω (related to frequency $f = 1/t_\omega$) and a strain amplitude ε_A . The resulted stress $\sigma(t)$ and phase difference δ between stress and strain were measured and fitted by $\sigma(t) = \sigma_0 + \sigma_A \sin(2\pi t/t_\omega + \delta)$. The storage and loss moduli were calculated by $E' = \sigma_A/\varepsilon_A \cos(\delta)$ and $E'' = \sigma_A/\varepsilon_A \sin(\delta)$, respectively. A strain amplitude $\varepsilon_A = 0.6\%$ was applied in all MD-DMS, which ensured deformations in the linear response regime.

Experiments - The $\text{Al}_{90}\text{Sm}_{10}$ MG was prepared by spinning-quenching techniques (see Supplemental Material [41] for details). The relaxation dynamics of the MG was studied by a dynamical mechanical analyzer using liquid Nitrogen for temperature control, which allows us to reach the cryogenic temperature (down to 150K). The measurements were conducted during a temperature ramping of 3 K/min together with a film tension oscillation using the discrete testing frequencies of 0.5, 2, 4, 8 and 16 Hz. The storage (E') and loss (E'') moduli were recorded for subsequent analysis and comparing with MD-DMS results.

Predictions by simulations - Figure 1 shows MD-DMS results by plotting the storage (E') and loss moduli (E'') as a function of temperature under different oscillation periods. The temperature-dependent loss modulus curves are fitted with a serial of Gaussian peaks which correspond to different relaxation processes. With the longest oscillation period $t_\omega = 1\mu\text{s}$ in Fig. 1, the loss modulus exhibits a broad peak in the temperature range from 200 K to 500 K, which corresponds to the typical β relaxation. We note that there exists no such pronounced peak of β relaxation in any previous MD simulations where only shoulder-like or excess wings were observed. At higher temperature, the dominant primary (α) relaxation peak shows a strong shoulder in the temperature range 500-600 K, which needs an extra peak function for the fitting. Considering this process decreases in amplitude as frequency increases (or t_ω decrease), which is

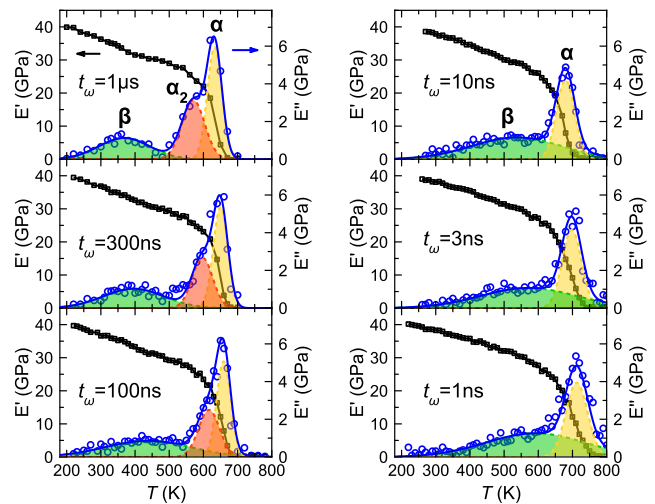


FIG. 1. Relaxation behaviors by simulations. Storage E' and loss E'' moduli of $\text{Al}_{90}\text{Sm}_{10}$ MG at different oscillations periods t_ω ranging from $1\mu\text{s}$ to 1ns . The loss moduli are fitted by multiple Gaussian functions.

consistent with behaviors of α relaxation in general, this new peak is named as α_2 process.

As shown in Fig. 1, with the decrease of oscillation period, all three peaks, α , α_2 and β , shift towards higher temperature. The α_2 peak gradually collapses in the α peak so that one can hardly differentiate them when t_ω is smaller than 10ns . With very short oscillation period (e.g. $t_\omega = 1\text{ns}$), the β peak also largely overlaps with the α peak. Thus, the simulations predict a complex relaxation scenario in the $\text{Al}_{90}\text{Sm}_{10}$ MG: at suitably long time scales (e.g., $1\mu\text{s}$) it has a pronounced β peak and an anomalous α_2 process in addition to the α relaxation.

Experimental verification - We next validate these computational predictions by DMS experiments for the as-quenched $\text{Al}_{90}\text{Sm}_{10}$ samples. Even though our longest simulation period reaches $1\mu\text{s}$, it is still about 5-6 orders of magnitude faster than the typical DMS experiments in which probing timescales are 0.1 – 10s. Extrapolating the temperature-time relation for the β relaxation from simulations to the experimental timescale leads to a characteristic temperature about 200 K (inset of Fig. 2(a)).

Figure 2(a) shows the experimental $E''(T)$ for the MG from a cryogenic DMS measurement at the testing frequency of 8 Hz. Remarkably, it clearly shows a pronounced β relaxation peak at about 220 K, consistent with the extrapolation of MD simulations. Figure 2(b) shows $E''(T)$ for more different testing frequencies. The peak temperature of the β relaxation increases with higher frequency (or shorter time period), which is also quantitatively agree with the MD simulations as shown in the inset of Fig. 2(a).

Besides, a close examination of $E''(T)$ curve in Fig. 2(a) indicates that there is notable excess contribution to the α relaxation around $T = 380\text{K}$, which

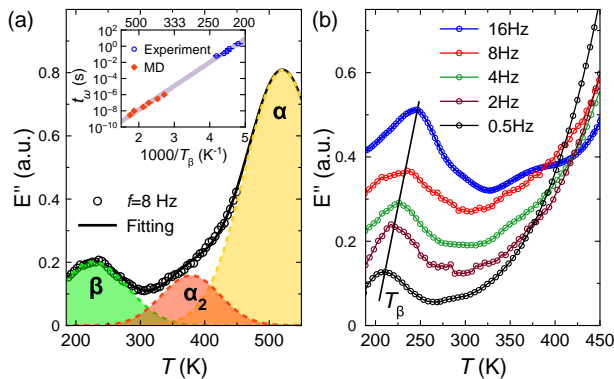


FIG. 2. Experimental DMS for Al₉₀Sm₁₀ MG. (a) DMS measured at the frequency 8 Hz and (b) at different frequencies as indicated. The inset in (a) shows the Arrhenius fitting of β relaxation peaks and DMS periods from both simulations and experiments. The fitting of α relaxation peak is to guide eyes. It is based on the extrapolation of simulation data at the experimental temperature, see details in Supplemental Material [41].

is corresponding well with the α_2 relaxation found from MD-DMS (Fig. 1). This α_2 process can also be discerned from different testing frequencies in Fig. 2(b). For example, it is more evident on the curve with the frequency of 16 Hz. Due to close coupling with α relaxation, α_2 process is more difficult to be resolved than the pronounced β relaxation. Nevertheless, its time-temperature relation can still be determined and compared favorably with MD simulations (see Supplemental Material [41]). Therefore, the presence of α_2 process in the MG could be ascertained with the guidance of MD simulation. Unfortunately, because of the occurrence of strong devitrification process in the current MG system [32], one cannot fully access the α relaxation peak at experimental timescales, resulting in the termination of experimental data at 450K.

Mechanism for β peak - The above experiments validate the predictions from MD simulations. Now we are in position to investigate the mechanisms of these complex relaxation processes. Recently, the structural rearrangements governing the β relaxations have been investigated in a model Ni₈₀P₂₀ MG [45] and a Y₆₅Cu₃₅ MG [46], which suggests string-like motions might be the origin of β relaxation. However, these MGs do not show such clear β relaxation peak as the Al₉₀Sm₁₀ at MD accessible timescales. One feature about string-like motions is that a particle jumps to a position that was occupied previously by another particle [45]. Structurally, this would result in a multi-peak curve for the distribution $p(u)$ of atomic displacements u during the deformation period, which is clearly observed in the present MG as shown in Fig. 3(a) (the mathematical definitions of displacement u and string-like motion are provided in Supplemental Material S3 [41]). The fact that the second and third peaks of $p(u)$ match exactly the first and second peaks of pair

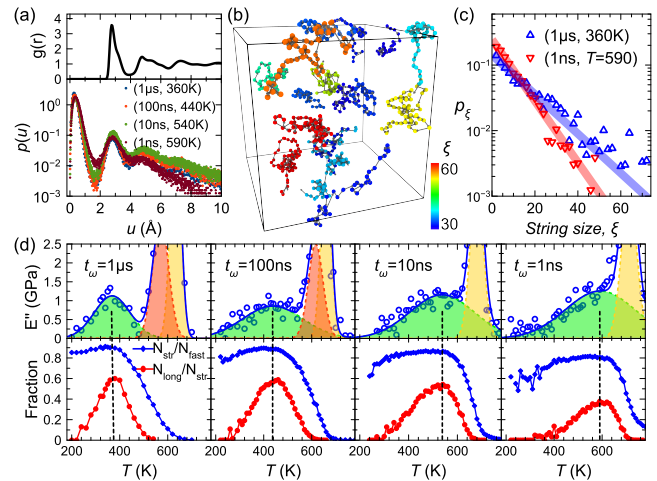


FIG. 3. String-like motion and β relaxation. (a) Upper panel shows the pair correlation function of Al₉₀Sm₁₀ MG at 300 K from MD simulation, while lower panel shows the probability of atomic displacement u at the condition of (t_ω, T_β) , where T_β is the peak temperature of β relaxation with the oscillation period t_ω . (b) String configurations at $T_\beta = 360$ K with $t_\omega = 1 \mu s$. The atoms in the strings with size $\xi < 30$ are removed for clarity. (c) The probability of string-like-moving atoms involved in the different sizes of strings at T_β with $t_\omega = 1 ns$ and $1 \mu s$, respectively. The lines indicate exponential fitting. (d) Relationship between β relaxation and string motion under four different oscillation periods from $1 \mu s$ to $1 ns$. The lower panel shows the fraction of string-like-moving atoms in the fast-moving atoms (N_{str}/N_{fast} , blue), and the fraction of atoms in the long string-like motions in the total string-like-moving atoms (N_{long}/N_{str} , red).

distribution function $g(r)$ at various β relaxation peaks in Fig. 3(a) indicates that atoms prefer to jumping to the position that is previously taken by another atom in its nearest or secondary neighbors, which further evidences string-like motions. Figure 3(b) shows that the strings can propagate in a rather large spatial range and form different types of geometries such as aggregations, loops and long-range chains. The string size ξ is defined by the number of atoms involved in the string. Figure 3(c) shows that the probability of the atom forming string follows an exponential function with the string size that can span up-to 70 atoms. While similar string-like motions were also observed in Lennard-Jones liquid model [47] and other systems [48, 49], the string size in the current Al₉₀Sm₁₀ is much longer than other systems. For example, the longest reported string in Ni₈₀P₂₀ contains 12 atoms [46] which is smaller by a factor 6 than current MG. Such long-range and large-scale string-like motion is a unique feature of the present MG which could be the reason for the uniquely pronounced β peak.

Figure 3(d) quantifies the fraction of string-like-moving atoms to the total number of fast-moving atoms (N_{str}/N_{fast}), as well as the fraction of atoms involved in the long-string motions to the total number of string-like-

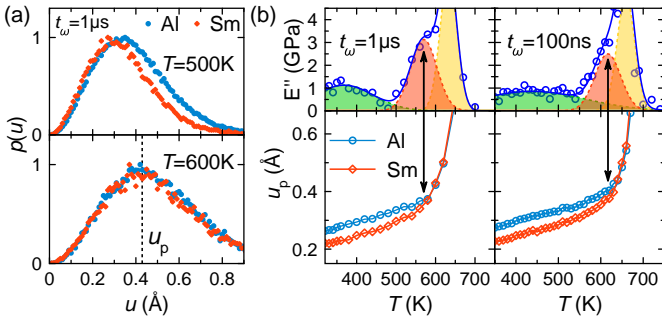


FIG. 4. Atomic motion decoupling and α_2 relaxation. (a) The probability of Al and Sm displacement with the oscillation period $t_\omega = 1\mu\text{s}$ at 500 K and 600 K, respectively. The dashed line indicates the peak position u_p . (b) u_p of Al and Sm atoms and loss moduli as a function of temperature for $t_\omega = 1\mu\text{s}$ and 100ns , respectively. The arrows highlight the transition points and the peak positions of α_2 relaxations.

moving atom ($N_{\text{long}}/N_{\text{str}}$) as a function of temperature. The long-string motion is defined by $\xi \geq 10$ here. The T -dependent loss moduli E'' are also plotted for comparison. One can see the peak of $N_{\text{long}}/N_{\text{str}}$ well matches the peak of β relaxation over all the studied oscillation periods t_ω . While the curve of $N_{\text{str}}/N_{\text{fast}}$ reaches a maximum plateau at the peak temperature of β relaxation T_β , $N_{\text{long}}/N_{\text{str}}$ manifests as a pronounced peak, whose position and width quantitatively agree with those of β relaxation peaks. Note this correlation does not change with the choice of long-string motion threshold (see Supplemental Material [41]). These results suggest long-string motions contribute more to the β relaxation than shorter ones, which emphasis the cooperative nature of β relaxation.

Mechanism for α_2 process - To grasp the microscopic origin of α_2 process, we analysis the probabilities $p(u)$ of atomic displacements u for Al and Sm atoms, respectively. As shown in Fig. 4(a), at a temperature $T = 500\text{K}$ lower than the peak of α_2 relaxations (about 560K), the peaks of $p(u)$ for Al and Sm separate with each other. While at the temperature higher than the α_2 process, the $p(u)$ peaks of Al and Sm well overlaps with each other. This comparison implies that decoupling of the motions of Al and Sm atoms occurs when the temperature crosses the α_2 peak.

To further quantify this behavior, Fig. 4(b) plots the most probable displacement, i.e. the peak position u_p of $p(u)$ as a function of temperature. When the temperature increases from the lower regime, u_p of Al and Sm atoms first increase separately until reaching a transition point where two curves merge to one. When comparing u_p with loss moduli in Fig. 4(b), we find that the transition point coincides with the peak position of α_2 relaxation over all the studied oscillation periods. Therefore, the α_2 relaxation well correlates with the dynamical transition from coupling to decoupling motions of Al and Sm atoms.

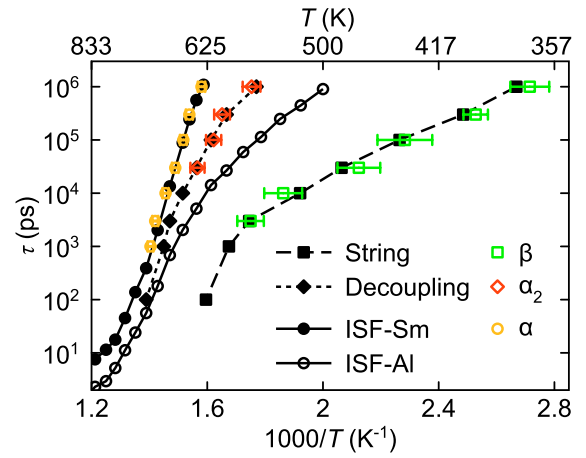


FIG. 5. Relaxation map of $\text{Al}_{90}\text{Sm}_{10}$ MG. ISF-Sm/Al: the α -relaxation time of Sm/Al atoms based on the Sm/Al ISF spectra. Decoupling: the transition temperature from coupled to decoupled most probable motions $u_p(T)$ of Al and Sm atoms. String: the most probable temperature to form the long-string motions.

It indicates the asynchronous freezing of fast and slow motions could be the key factor leading to this process.

In Fig. 5, we summarized all the studied processes in a relaxation map over a wide range of temperature and timescales. One can see that the α_2 relaxation and the decoupling between Sm and Al atoms follow the same temperature-time relation, suggesting an intrinsic correlation between them. Meanwhile, the β relaxation and the long string-like motions ($\xi \geq 10$) agree with each other. Hence, the atomistic simulations not only predicted the complex relaxations in the MGs, but also elucidate the underlying mechanisms for them.

Figure 5 also reveals that the $\text{Al}_{90}\text{Sm}_{10}$ MG is a typical glass system in which the solute and solvent elements show dramatically different dynamical behaviors: the α relaxation time calculated based on the intermediate scattering function (ISF) of Sm atoms are orders of magnitudes longer than the Al atoms (see details in Supplemental Material [41]). Moreover, the global α relaxation determined from MD-DMS correlates only with the α relaxation time from the ISF of Sm atoms, implying that it is controlled predominately by the slowest process. Previous simulations [52–54] suggested that the large atomic size ratio disparity might cause more than one glass transitions in model systems. In a recent theoretical work, Cui *et al.* [50] pointed out that the dynamical decoupling between constituents with wide mass disparity might lead to a separated relaxation process and suggested it to be a β relaxation. The identified α_2 process here might be an experimental evidence for these scenarios in real glasses. Moreover, it indicates that the related process can be an additional primary process in stead of β relaxation. Finally, we note that the α_2 process

might not be unique to the Al₉₀Sm₁₀ MGs: in a recent work Xue *et al.* [51] reported the relaxation processes in a series of LaGa-based MGs. Although not discussed explicitly, their data indeed exhibit a discernable α_2 -like process, which may also be related to the mobility decoupling between fast Ga and slow La atoms.

We have shown that with atomic simulations, one could predict complex relaxation processes in MGs at the laboratory timescales and clarify their microscopic origins. A MG system with previously unidentified α_2 relaxation process due to the mobility decoupling and strong β relaxations caused by long-string motions has thus been predicted by simulations and verified by experiments. The combined experiments (validations) and simulations (predictions and clarification of mechanisms) represent a first glimpse of what may become a routine and integrated step in the study of glass relaxation. With above interpretations, one would expect an abundant α_2 relaxations, or even more relaxation processes in glass states. It then suggests that efforts aimed at a quantitative theory to predict glass relaxation would be desirable. The results presented above thus open new challenges and opportunities for furthering our understanding of glass relaxations.

Acknowledgements We thank Ms. Xiao-Hui Qin for experimental help. The work at HUST are supported by National Science Foundation of China (NSFC 51601064) and the Thousands of Young Talent Program. Work at Ames Laboratory was supported by the U.S. Department of Energy (DOE), Office of Science, Basic Energy Sciences, Materials Science and Engineering Division, under Contract No. DE-AC02-07CH11358, including a grant of computer time at the National Energy Research Supercomputing Center (NERSC) in Berkeley, CA.

* These authors contributed equally.

† Email: haibinyu@hust.edu.cn

- [1] L. Berthier and G. Biroli, *Rev. Mod. Phys.* **83**, 587 (2011).
- [2] C. A. Angell, K. L. Ngai, G. B. McKenna, P. F. McMillan, and S. W. Martin, *J. Appl. Phys.* **88**, 3113 (2000).
- [3] M. Micoulaut, *Rep. Prog. Phys.* **79**, 066504 (2016).
- [4] P. Lunkenheimer, U. Schneider, R. Brand, and A. Loidl, *Contemp. Phys.* **41**, 15 (2000).
- [5] S. Khodadadi and A. P. Sokolov, *Soft Matter* **11**, 4984 (2015).
- [6] B. A. Pazmiño Betancourt, P. Z. Hanakata, F. W. Starr, and J. F. Douglas, *Proc. Natl. Acad. Sci. U.S.A.* **112**, 2966 (2015).
- [7] Y. Lahini, O. Gottesman, A. Amir, and S. M. Rubinstein, *Phys. Rev. Lett.* **118**, 085501 (2017).
- [8] H. B. Yu, W. H. Wang, H. Y. Bai, and K. Samwer, *Natl. Sci. Rev.* **1**, 429 (2014).
- [9] H.-B. Yu, W.-H. Wang, and K. Samwer, *Mater. Today* **16**, 183 (2013).
- [10] K. L. Ngai and M. Paluch, *J. Chem. Phys.* **120**, 857 (2004).
- [11] S. Capaccioli, M. Paluch, D. Prevosto, L.-M. Wang, and K. L. Ngai, *J. Phys. Chem. Lett.* **3**, 735 (2012).
- [12] K. Geirhos, P. Lunkenheimer, and A. Loidl, *Phys. Rev. Lett.* **120**, 085705 (2018).
- [13] J. Sondhauß, M. Lantz, B. Gotsmann, and A. Schirmeisen, *Langmuir* **31**, 5398 (2015).
- [14] R. C. Welch, J. R. Smith, M. Potuzak, X. Guo, B. F. Bowden, T. J. Kiczanski, D. C. Allan, E. A. King, A. J. Ellison, and J. C. Mauro, *Phys. Rev. Lett.* **110**, 265901 (2013).
- [15] S. Kuchemann and R. Maass, *Scr. Mater.* **137**, 5 (2017).
- [16] P. Luo, P. Wen, H. Y. Bai, B. Ruta, and W. H. Wang, *Phys. Rev. Lett.* **118**, 225901 (2017).
- [17] Q. Wang, S. T. Zhang, Y. Yang, Y. D. Dong, C. T. Liu, and J. Lu, *Nat. Commun.* **6**, 7876 (2015).
- [18] Y. Yu, M. Wang, M. M. Smedskjaer, J. C. Mauro, G. Sant, and M. Bauchy, *Phys. Rev. Lett.* **119**, 095501 (2017).
- [19] D. Cangialosi, V. M. Boucher, A. Alegria, and J. Colmenero, *Phys. Rev. Lett.* **111**, 095701 (2013).
- [20] B. Ruta, Y. Chushkin, G. Monaco, L. Cipelletti, E. Pineda, P. Bruna, V. M. Giordano, and M. Gonzalez-Silveira, *Phys. Rev. Lett.* **109**, 165701 (2012).
- [21] Q. Wang, J. J. Liu, Y. F. Ye, T. T. Liu, S. Wang, C. T. Liu, J. Lu, and Y. Yang, *Mater. Today* **20**, 293 (2017).
- [22] B. Ruta, E. Pineda, and Z. Evenson, *J. Phys. Condens. Matter* **29**, 503002 (2017).
- [23] Q. L. Bi, Y. J. Lu, and W. H. Wang, *Phys. Rev. Lett.* **120**, 155501 (2018).
- [24] H. B. Yu, K. Samwer, W. H. Wang, and H. Y. Bai, *Nat. Commun.* **4**, 2204 (2013).
- [25] V. M. Giordano and B. Ruta, *Nat. Commun.* **7**, 10344 (2016).
- [26] B. Wang, B. S. Shang, X. Q. Gao, W. H. Wang, H. Y. Bai, M. X. Pan, and P. F. Guan, *J. Phys. Chem. Lett.* **7**, 4945 (2016).
- [27] Y. Q. Cheng, E. Ma, and H. W. Sheng, *Phys. Rev. Lett.* **102**, 245501 (2009).
- [28] Y. Q. Cheng and E. Ma, *Prog. Mater. Sci.* **56**, 379 (2011).
- [29] Y. He, P. Yi, and M. L. Falk, *Phys. Rev. Lett.* **122**, 035501 (2019).
- [30] M. I. Mendeleev, F. Zhang, Z. Ye, Y. Sun, M. C. Nguyen, S. R. Wilson, C. Z. Wang, and K. M. Ho, *Model. Simul. Mater. Eng.* **23**, 045013 (2015).
- [31] Y. Sun, Y. Zhang, F. Zhang, Z. Ye, Z. Ding, C.-Z. Wang, and K.-M. Ho, *J. Appl. Phys.* **120**, 015901 (2016).
- [32] Z. Ye, F. Zhang, Y. Sun, M. C. Nguyen, S. H. Zhou, L. Zhou, F. Meng, R. T. Ott, E. Park, M. F. Besser, M. J. Kramer, Z. J. Ding, M. I. Mendeleev, C. Z. Wang, R. E. Napolitano, and K. M. Ho, *Phys. Rev. Materials* **1**, 055601 (2017).
- [33] L. Yang, F. Zhang, F.-Q. Meng, L. Zhou, Y. Sun, X. Zhao, Z. Ye, M. J. Kramer, C.-Z. Wang, and K.-M. Ho, *Acta Mater.* **156**, 97 (2018).
- [34] L. Wang, J. Hoyt, N. Wang, and N. Provatas, *arXiv* **1810.05298** (2018).
- [35] Y. Sun, F. Zhang, L. Yang, H. Song, M. I. Mendeleev, C.-Z. Wang, and K.-M. Ho, *Phys. Rev. Materials* **3**, 023404 (2019).
- [36] L. Zhao, G. B. Bokas, J. H. Perepezko, and I. Szlufarska, *Acta Mater.* **142**, 1 (2018).
- [37] H.-B. Yu and K. Samwer, *Phys. Rev. B* **90**, 144201 (2014).

- [38] W. M. Brown, P. Wang, S. J. Plimpton, and A. N. Tharrington, *Comp. Phys. Comm.* **182**, 898 (2011).
- [39] W. M. Brown, A. Kohlmeyer, S. J. Plimpton, and A. N. Tharrington, *Comp. Phys. Comm.* **183**, 449 (2012).
- [40] W. M. Brown and Y. Masako, *Comp. Phys. Comm.* **184**, 2785 (2013).
- [41] See Supplemental Material [url] for technical details of simulations and experiments, the calculation details of string-like motions and the detailed intermediate scatter functions, which includes Refs. [42-44].
- [42] Z. Ye, F. Zhang, Y. Sun, M. C. Nguyen, S. H. Zhou, L. Zhou, F. Meng, R. T. Ott, E. Park, M. F. Besser, M. J. Kramer, Z. J. Ding, M. I. Mendelev, C. Z. Wang, R. E. Napolitano, and K. M. Ho, *Phys. Rev. Materials* **1**, 055601 (2017).
- [43] J. Horbach and W. Kob, *Phys. Rev. E* **64**, 041503 (2001).
- [44] J.-P. Hansen and I. R. McDonald, *Theory of Simple Liquids*, 3rd ed. (Academic Press, London, 2006).
- [45] H.-B. Yu, R. Richert, and K. Samwer, *Sci. Adv.* **3**, e1701577 (2017).
- [46] H.-B. Yu, M.-H. Yang, Y. Sun, F. Zhang, J.-B. Liu, C. Z. Wang, K. M. Ho, R. Richert, and K. Samwer, *J. Phys. Chem. Lett.* **9**, 5877 (2018).
- [47] C. Donati, J. F. Douglas, W. Kob, S. J. Plimpton, P. H. Poole, and S. C. Glotzer, *Phys. Rev. Lett.* **80**, 2338 (1998).
- [48] F. W. Starr, J. F. Douglas, and S. Sastry, *J. Chem. Phys.* **138**, 12A541 (2013).
- [49] H. Zhang, C. Zhong, J. F. Douglas, X. Wang, Q. Cao, D. Zhang, and J.-Z. Jiang, *J. Chem. Phys.* **142**, 164506 (2015).
- [50] B. Cui, Z. Evenson, B. Fan, M.-Z. Li, W.-H. Wang, and A. Zacccone, *Phys. Rev. B* **98**, 144201 (2018).
- [51] R. J. Xue, L. Z. Zhao, B. Zhang, H. Y. Bai, W. H. Wang, and M. X. Pan, *Appl. Phys. Lett.* **107**, 241902 (2015).
- [52] Th. Voigtmann and J. Horbach, *Phys. Rev. Lett.* **103**, 205901 (2009).
- [53] H. W. Cho, G. Kwon, B.J. Sung, and A.Yethiraj, *Phys. Rev. Lett.* **109**, 155901 (2012).
- [54] J. Bosse and Y. Kaneko, *Phys. Rev. Lett.* **74**, 4023 (1995).